



UNIVERSITÀ  
DEGLI STUDI  
DI TRIESTE

# Fast and accurate excitation and CD spectra of large systems with PolTDDFT: from molecular to plasmonic regimes

Mauro Stener

*Dipartimento di Scienze Chimiche e Farmaceutiche, Università di Trieste, Italy*  
*stener@units.it*

AMS2022 Webinar series (fall)  
October 28<sup>th</sup> 2022

## PolTDDFT: why yet another TDDFT scheme?

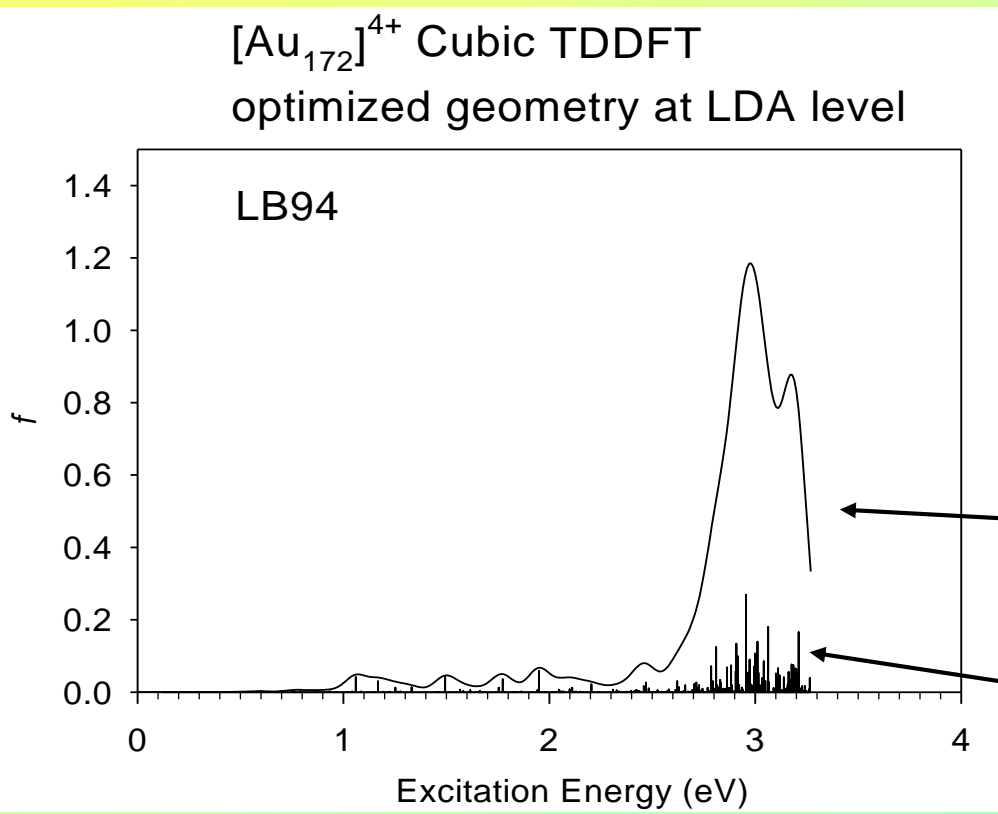
**Theory:** for large metal nanoclusters (up to 1000 atoms) TDDFT is the only possibility!

1. **Efficiency:** the polTDDFT is an alternative to **Casida** scheme, avoid **Davidson diagonalization!** Very competitive when too many excited states are needed.
2. **Accuracy/Efficiency:** **Hybrid** functionals (B3LYP), new **Hybrid Diagonal Approximation (HDA)**
3. **Accuracy/Efficiency:** optimization of density **fitting basis** set.
4. **Validation:** comparison with experiment. Monolayer-Protected Cluster (**MPC**) structure and optical properties well characterized.
5. **Selected Applications:** dichroism in nanoplasmonics
6. **Input example/explanation**

# TDDFT Equations: Casida approach

$$\Omega \mathbf{F}_I = E_I^2 \mathbf{F}_I$$

Casida formulation: Diagonalization of  $\Omega$  matrix furnishes discrete excitation energies and intensities  $\text{dim} = N_{\text{occ}} * N_{\text{virt}}$



STO TZP, closed shell:

$$N_{\text{occ}} = 1632 \quad N_{\text{virt}} = 3872$$

$$\text{dim}(\Omega) = 6.3 \cdot 10^6$$

Gaussian broadening

TDDFT results, lowest  
 $n$  eigenvalues

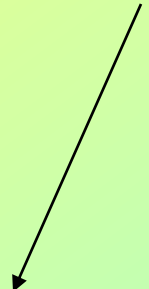
# Linear response : general theory

$$V_{EXT}(\vec{r}, \omega)$$

External TD perturbation, with  $\omega$  frequency (dipole)

$$\rho^{(1)}(\vec{r}, \omega) \text{ Induced density by the external field}$$

$$\rho^{(1)}(\vec{r}, \omega) = \int d\vec{r}' \chi(\vec{r}, \vec{r}', \omega) V_{EXT}(\vec{r}', \omega)$$



Dielectric susceptibility, not easy to calculate

# TDDFT: general theory

TDDFT: instead of  $\chi$ , use  $\chi_{KS}$  of a model system of non-interacting electrons and a modified external potential:  $V_{SCF}$

$$\rho^{(1)}(\vec{r}, \omega) = \int d\vec{r}' \chi_{KS}(\vec{r}, \vec{r}', \omega) V_{SCF}(\vec{r}', \omega)$$

*Coupled, but linear!*

$$V_{SCF}(\vec{r}, \omega) = V_{EXT}(\vec{r}, \omega) + \int d\vec{r}' \underbrace{\frac{\rho^{(1)}(\vec{r}', \omega)}{|\vec{r} - \vec{r}'|}}_{K(\vec{r}, \vec{r}')} + \underbrace{\frac{dV_{XC}^{LDA}(\rho(\vec{r}))}{d\rho(\vec{r})}}_{\text{non-local term}}$$

$K(\vec{r}, \vec{r}')$  (kernel)

## *Efficiency: polTDDFT direct (not iterative) algorithm*

Exploit linearity of the problem:

$$\delta V = K \rho^{(1)} \xrightarrow{\text{defines the kernel } K}$$

$$\rho^{(1)} = \chi_{KS} V_{SCF} \xrightarrow{\text{defines the susceptibility } \chi_{KS}}$$

$$V_{SCF} = V_{EXT} + \delta V$$

The Response Equation becomes:

$$\boxed{[1 - \chi_{KS} K] \rho^{(1)} = \chi_{KS} V_{EXT}}$$

$$\rho^{(1)} = \sum_{\mu}^{fit} b_{\mu} f_{\mu}$$

To solve : represent the response equation in the **auxiliary density fitting basis functions**, dimension of fitting set (**density-based** formulation). At variance with **density-matrix** Casida formulation. For  $[\text{Au}_{172}]^{4+}$   $\dim(1 - \chi_{KS} K) = 5848$  (instead of  $6.3 \cdot 10^6$  )!!!

# Extract the spectrum from polarizability:

$$\alpha_{pq}(\omega) = \int \rho_p^{(1)}(\omega, \bar{r}) q d\bar{r}$$

$$\alpha(\omega) = \frac{1}{3} \sum_{q=1}^3 \alpha_{qq}(\omega)$$

$$\sigma(\omega) = \frac{4\pi\omega}{c} \Im[\alpha(\omega)]$$

The first order density  $\rho^{(1)}$  calculated from TDDFT equations, for each photon energy  $\omega$  with  $\omega = \omega_R + i\omega_I$  the imaginary part corresponds to lorentzian HWHM broadening.  
basis set: auxiliary density fitting functions optimized for POLTTDFT must be employed!

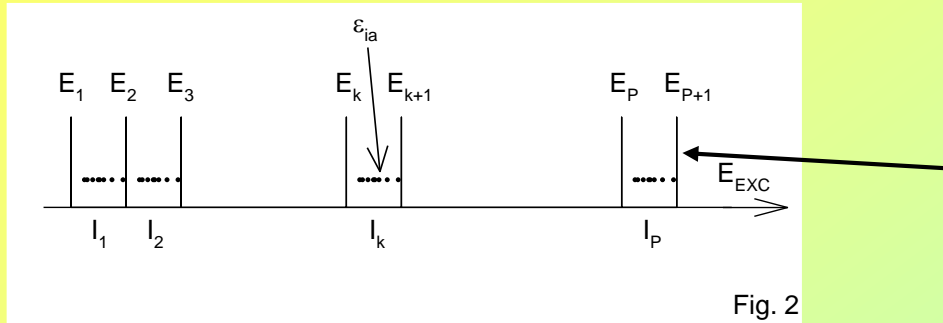
$$\rho^{(1)} = \sum_{\mu}^{fit} b_{\mu} f_{\mu}$$

$$[1 - \chi_{KS} K] \rho^{(1)} = \chi_{KS} V_{EXT} \quad [\mathbf{S} - \mathbf{M}(\omega)] \mathbf{b} = \mathbf{d}(\omega)$$

The “only” problem is to calculate efficiently  $\chi_{KS}$ !

# Change the double sum:

$$\chi_{KS}(\omega, \bar{r}, \bar{r}') = \sum_i^{N_{occ}} \sum_a^{N_{virt}} \varphi_i(\bar{r}) \varphi_a(\bar{r}) \frac{4\epsilon_{ia}}{\omega^2 - \epsilon_{ia}^2} \varphi_a(\bar{r}') \varphi_i(\bar{r}') = \sum_i^{N_{occ}} \sum_a^{N_{virt}} \Theta_{ia}(\bar{r}) \lambda_{ia}(\omega) \Theta_{ia}(\bar{r}')$$



**Cut-off** crucial input choice for polTDDFT: include relevant excitations but avoid unnecessary ones to prevent numerical errors propagation.

The energy grid consists of  $P+1$  knots:  $\{E_k\}_{k=1,\dots,P+1}$  and are defined  $P$  intervals:  $I_k = [E_k, E_{k+1}), k = 1, \dots, P$

Now it is possible to change the double sum of previous equation (13) as follows:

$$\chi_{KS}(\omega, \bar{r}, \bar{r}') = \sum_{k=1}^P \sum_{\epsilon_{ia} \in I_k} \Theta_{ia}(\bar{r}) \lambda_{ia}(\omega) \Theta_{ia}(\bar{r}')$$

$$\chi_{KS}(\omega, \bar{r}, \bar{r}') = \sum_{k=1}^P \frac{4\bar{E}_k}{\omega^2 - \bar{E}_k^2} \sum_{\epsilon_{ia} \in I_k} \Theta_{ia}(\bar{r}) \Theta_{ia}(\bar{r}')$$

## Build the matrix:

TDDFT equation:

$$[\mathbf{S} - \mathbf{M}(\omega)]\mathbf{b} = \mathbf{d}(\omega)$$

$$M(\omega)_{\mu\nu} = \sum_{k=1}^P s_k(\omega) \sum_{\varepsilon_{ia} \in I_k} \langle f_\mu | \Theta_{ia}(\bar{r}) \rangle \langle \Theta_{ia}(\bar{r}') | K | f_\nu \rangle = \sum_{k=1}^P s_k(\omega) G_{\mu\nu}^k$$

$$s_k(\omega) = \frac{4\bar{E}_k}{\omega^2 - \bar{E}_k^2}$$

With this scheme, the **M** matrix is calculated at each photon energy  $\omega$ , simply as a linear combination of matrices  $\mathbf{G}^k$  with coefficients  $s_k(\omega)$ .

The calculation of  $\chi_{KS}$  is fast (just sum of matrices) and small (over the fitting functions)!

Approximations: imaginary broadening and energy discretization.

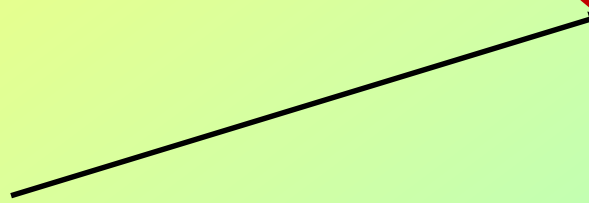
# Accuracy/Efficiency: Hybrid Diagonal Approximation (HDA)

To introduce HDA is convenient to start from RPA equations:

$$\begin{pmatrix} A & B \\ B^* & A^* \end{pmatrix} \begin{pmatrix} X \\ Y \end{pmatrix} = \omega \begin{pmatrix} 1 & 0 \\ 0 & -1 \end{pmatrix} \begin{pmatrix} X \\ Y \end{pmatrix}$$

For hybrid kernels the matrix elements takes this form,  $\alpha$  fraction of non-local exchange

$$A_{ia,jb} = \delta_{ij}\delta_{ab}(\varepsilon_a - \varepsilon_i) + \langle aj|ib\rangle - \alpha\langle aj|bi\rangle + (1-\alpha)\langle a|\frac{\partial V_{xc}}{\partial \rho} j^* b|i\rangle$$



Kernel non-local exchange elements: very demanding when non-gaussian basis are employed!

# Hybrid Diagonal Approximation (HDA)

HDA consists to consider only the **diagonal** exchange elements:

$$A_{ia,jb} = \delta_{ij}\delta_{ab}(\varepsilon_a - \varepsilon_i - \Delta_{ia}) + \langle aj|ib\rangle + \langle a|\frac{\partial V_{xc}}{\partial \rho} j^* b|i\rangle$$

$$\Delta_{ia} = \alpha\langle ai|ai\rangle + \alpha\langle a|\frac{\partial V_{xc}}{\partial \rho} i^* a|i\rangle$$

The **diagonal** exchange elements are few and cheap to calculate, even for non-gaussian basis set. At present calculated numerically. Next release AMS2023: also calculated analytically with fitting (Resolution of the Identity) (Pierpaolo D'Antoni TCCM master thesis, paper in preparation). Speedup factor of 30 by RI!!!

HDA is a general approximation, it has been implemented (AMS2021) for both Casida and polTDDFT algorithms!

# Hybrid Diagonal Approximation (HDA)

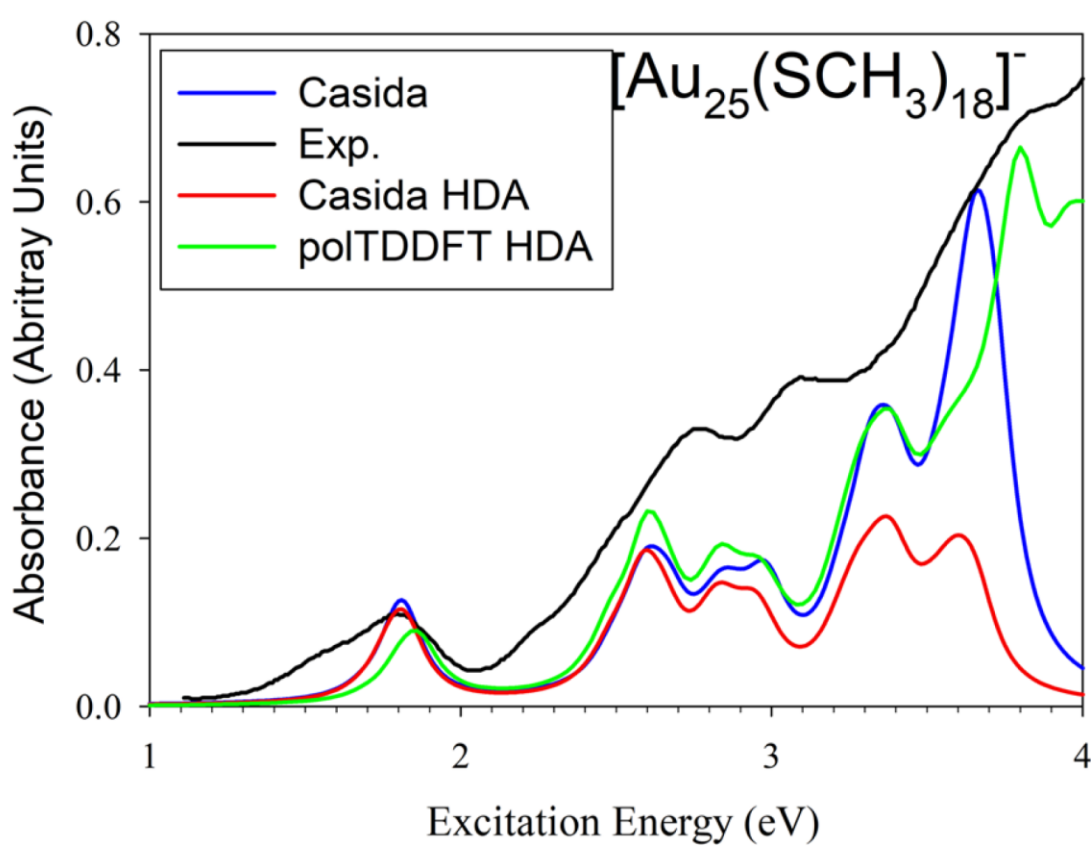


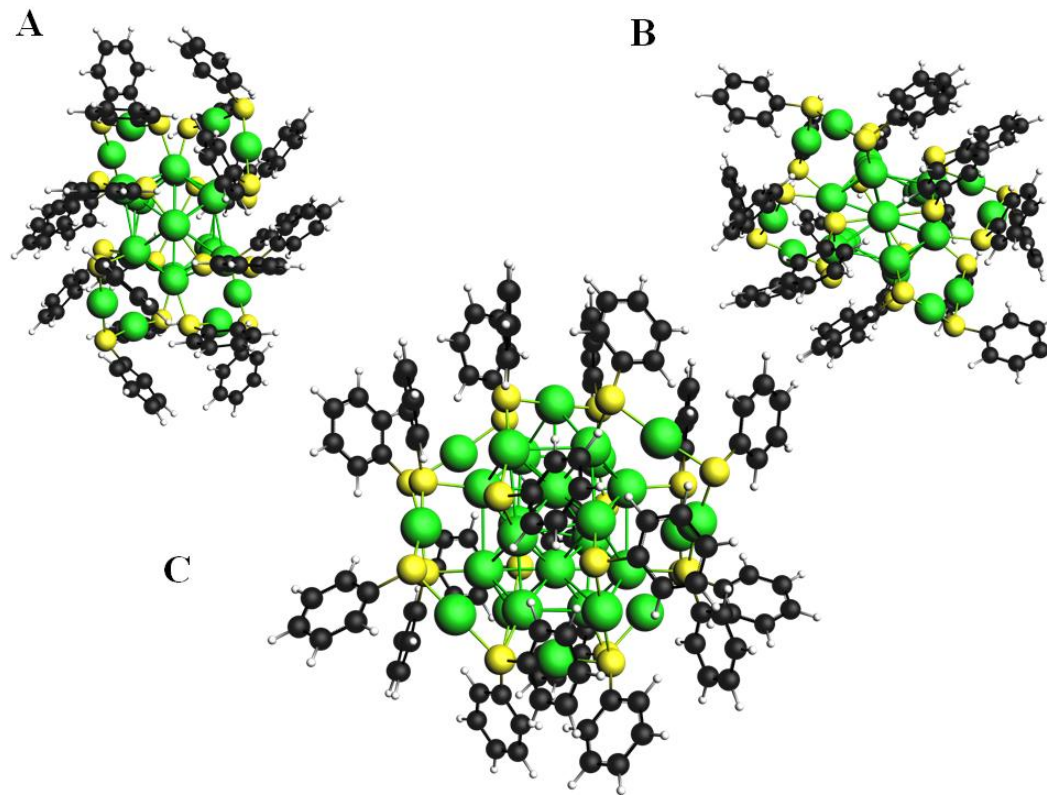
**FIG. 3.** Valence excitation spectra of  $[\text{Au}_{25}(\text{SCH}_3)_{18}]^-$ . Calculated profile with the Casida approach (blue line), Casida HDA (red line), and polTDDFT (green line), broadened with HWHM = 0.075 eV and experimental data<sup>37</sup> (black line).

**Timing (24 cores)**  
**Casida:** 61 h up 3.7 eV  
**Casida HDA:** 9 h up 3.7 eV  
**polTDDFT:** 16 h up to 5eV

Hardware: HP ProLiant DL580 Gen10 server Intel®Xeon®Gold 6140 CPU @ 2.30 GHz, 728 GB of RAM

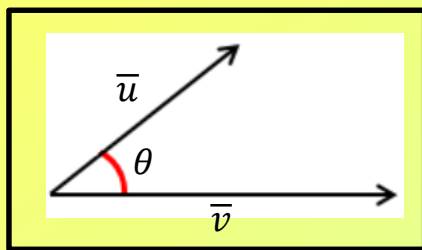
# Hybrid Diagonal Approximation (HDA)

	$[\text{Au}_{25}(\text{SCH}_3)_{18}]^-$	$\text{Au}_{28}(\text{SC}_6\text{H}_5)_{20}$
Atoms	115	268
polTDDTFT HDA numerical	16h	84h
polTDDTFT HDA fitted		3h

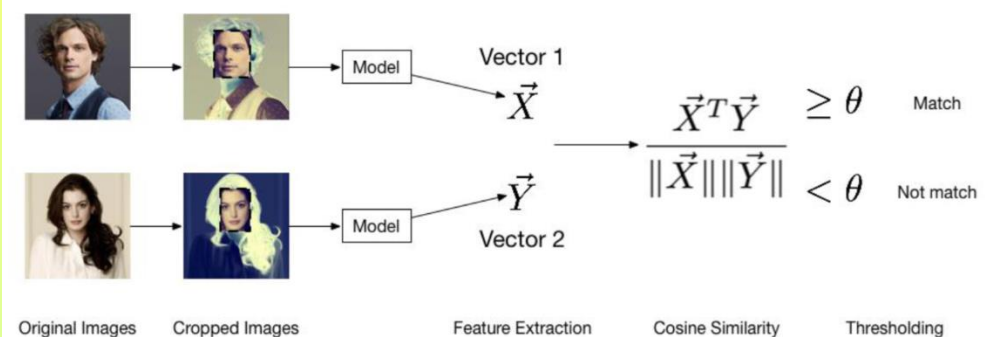


# Efficiency/Accuracy: POLTDDFT fitting basis set

$$\bar{v} \cdot \bar{u} = |\bar{v}| |\bar{u}| \cos(\theta) \Rightarrow \cos(\theta) = \frac{\bar{v} \cdot \bar{u}}{|\bar{v}| |\bar{u}|}$$



}



1 H	2 He															
Hydrogen 1.008	Helium 4.003															
3 Li	4 Be															
Lithium 6.941	Beryllium 9.012															
11 Na	12 Mg															
Sodium 22.990	Magnesium 24.305															
19 K	20 Ca															
Potassium 39.098	Calcium 40.078															
37 Rb	38 Sr															
Rubidium 85.468	Samarium 137.328															
55 Cs	56 Ba															
Cesium 132.905	Boron 226.025															
87 Fr	88 Ra															
Francium 223.020	Radium 226.025															
21 Sc	22 Ti	23 V	24 Cr	25 Mn	26 Fe	27 Co	28 Ni	29 Cu	30 Zn	31 Ga	32 Ge	33 As	34 Se	35 Br	36 Kr	
Scandium 44.956	Titanium 47.867	Vanadium 50.942	Chromium 51.996	Manganese 54.938	Iron 55.845	Cobalt 56.933	Nickel 56.693	Copper 59.546	Zinc 65.38	Gallium 69.723	Silicon 72.61	Phosphorus 74.932	Germanium 78.971	Bromine 79.904	Krypton 83.796	
39 Y	40 Nb	41 Mo	42 Tc	43 Ru	44 Rh	45 Pd	46 Ag	47 Cd	48 In	49 Sn	50 Te	51 Sb	52 I	53 Po	54 At	55 Rn
Yttrium 88.906	Niobium 91.224	Molybdenum 92.906	Rhenium 95.95	Techneium 96.907	Ruthenium 101.07	Rhodium 102.996	Palladium 106.42	Cadmium 112.414	Inium 114.818	Tin 118.711	Tellurium 121.780	Iodine 126.904	Astatine 131.294	Polonium 208.982	Astaine 209.987	Radon 222.018
57-71	72	73	74	75	76	77	78	79	80	81	82	83	84	85	86	87
Hafnium 178.49	Tantalum 180.948	Tungsten 183.84	Rhenium 186.207	Osmium 190.23	Irindium 192.217	Platinum 195.085	Gold 196.967	Mercury 200.592	Thallium 204.383	Lead 207.2	Bismuth 208.980	Poison 208.982	Polonium 208.982	Astatine 209.987	Radon 222.018	Fracton 223.020
89-103																
Lanthanide Series	57 La	58 Ce	59 Pr	60 Nd	61 Pm	62 Sm	63 Eu	64 Gd	65 Tb	66 Dy	67 Ho	68 Er	69 Tm	70 Yb	71 Lu	
	Lanthanum 138.905	Cerium 140.116	Praseodymium 140.908	Neodymium 144.243	Promethium 144.913	Samarium 150.36	Europium 151.964	Gadolinium 157.25	Terbium 158.925	Dysprosium 162.500	Holmium 164.930	Erbium 167.259	Thulium 168.934	Ytterbium 173.055	Lucretium 174.967	
Actinide Series	89 Ac	90 Th	91 Pa	92 U	93 Np	94 Pu	95 Am	96 Cm	97 Bk	98 Cf	99 Es	100 Fm	101 Md	102 No	103 Lr	
	Actinium 227.028	Thorium 232.038	Protactinium 231.036	Uranium 238.029	Neptunium 237.048	Plutonium 244.064	Americium 243.061	Curium 247.070	Berkelium 247.070	Californium 251.080	Einsteinium 254.0	Fermium 257.995	Mendeleyium 258.1	Nobelium 259.101	Lawrencium 262.0	

- 73 elements of the periodic table approx. 2 millions spectra analyzed

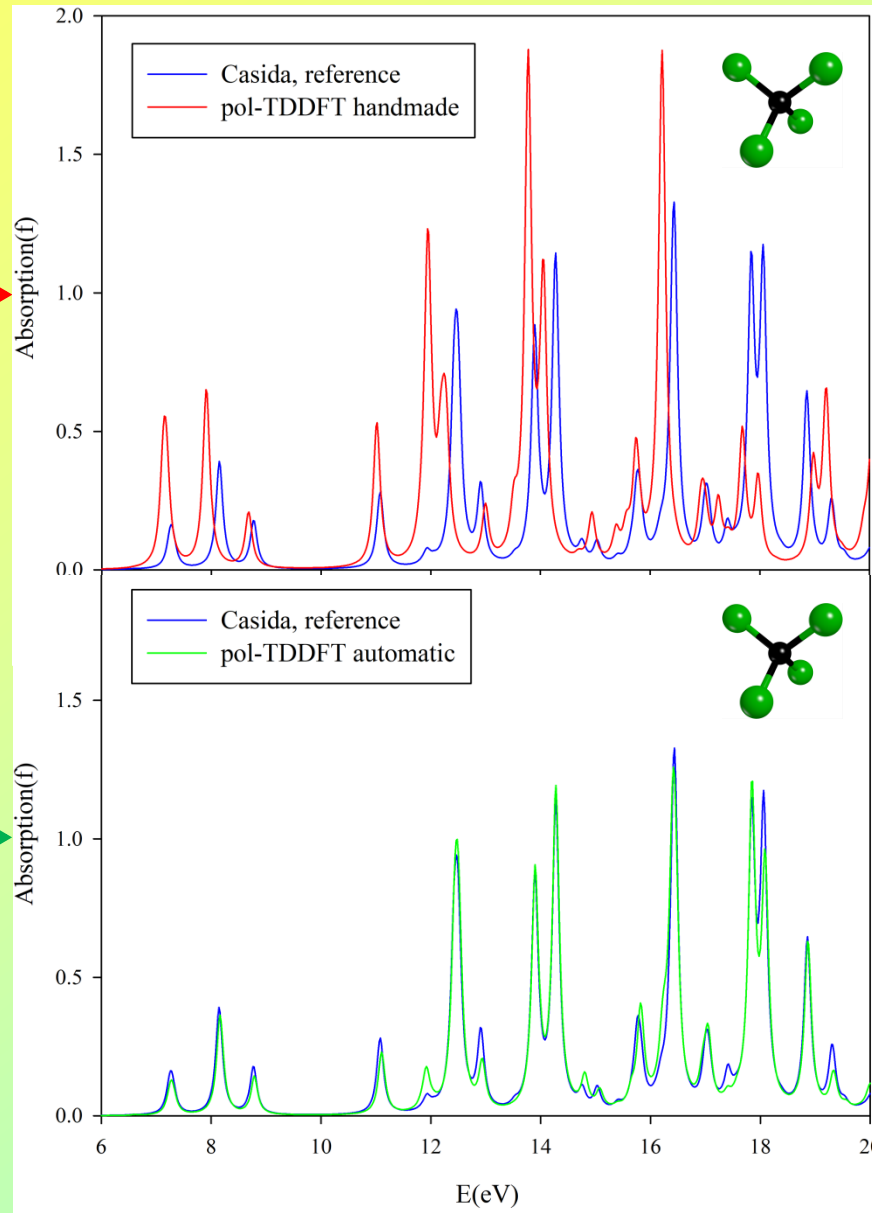
- High spread of the pol-TDDFT method in particular for “large” systems

- High accuracy and robustness included in AMS-2021

# Density fitting basis

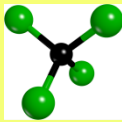
Frozen core Cl.2p TZP ZORA, 26 functions

1S	$\alpha=29.10$
2S	$\alpha=29.57$
2S	$\alpha=18.51$
3S	$\alpha=17.08$
3S	$\alpha=11.50$
4S	$\alpha=10.27$
4S	$\alpha=7.25$
4S	$\alpha=5.12$
5S	$\alpha=4.51$
5S	$\alpha=3.29$
5S	$\alpha=2.40$
2P	$\alpha=21.25$
3P	$\alpha=16.90$
4P	$\alpha=13.28$
4P	$\alpha=8.31$
5P	$\alpha=6.53$
5P	$\alpha=4.28$
5P	$\alpha=2.80$
3D	$\alpha=16.31$
4D	$\alpha=12.49$
4D	$\alpha=7.62$
5D	$\alpha=5.86$
5D	$\alpha=3.75$
5D	$\alpha=2.40$
4F	$\alpha=5.00$
4F	$\alpha=3.00$
5G	$\alpha=3.50$

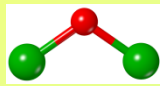


# Descriptors: match with respect to Casida reference

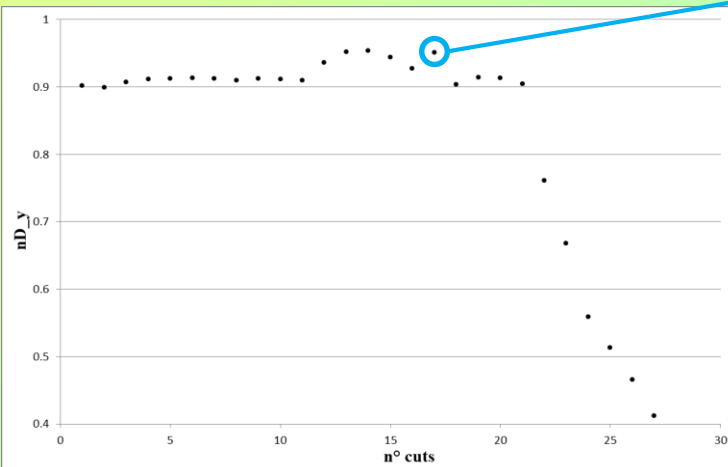
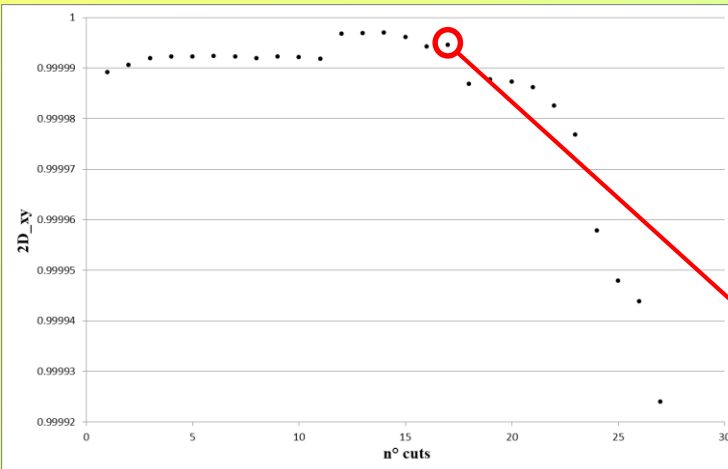
$CCl_4$



$Cl_2O$



$HCl$

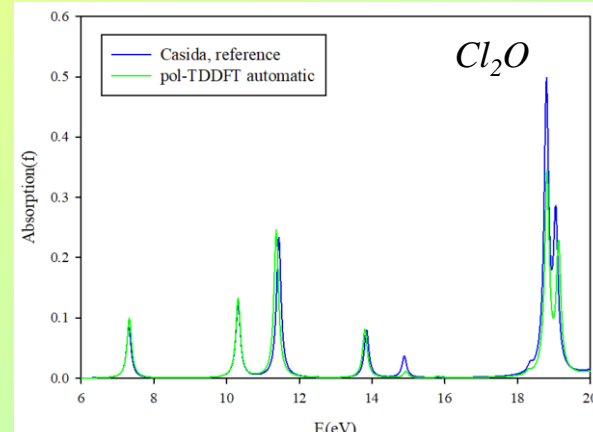
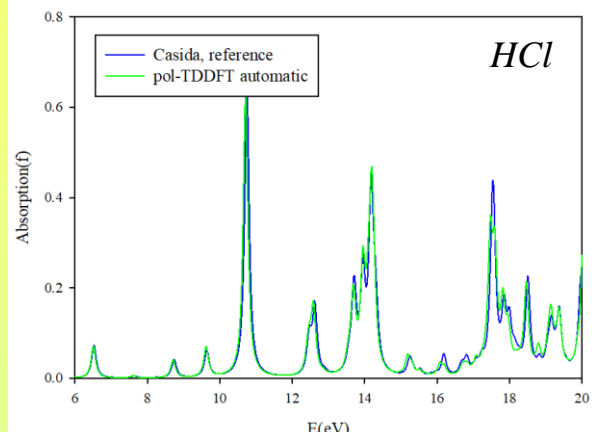
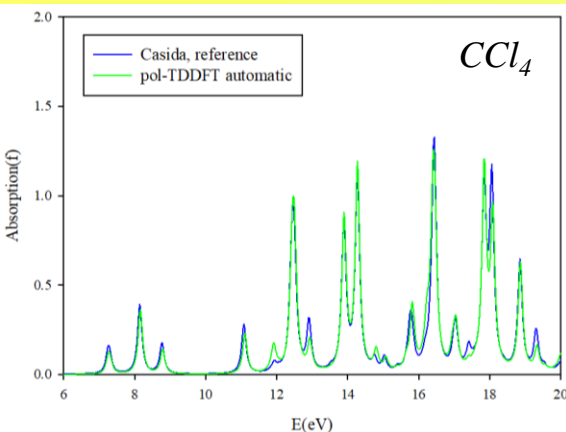


Result

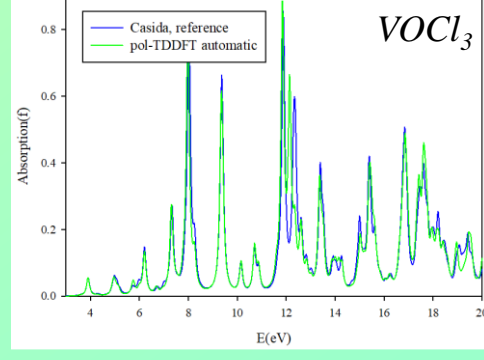
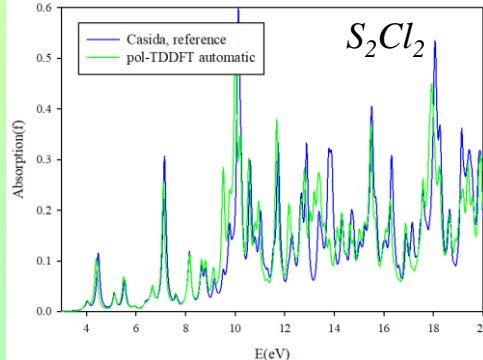
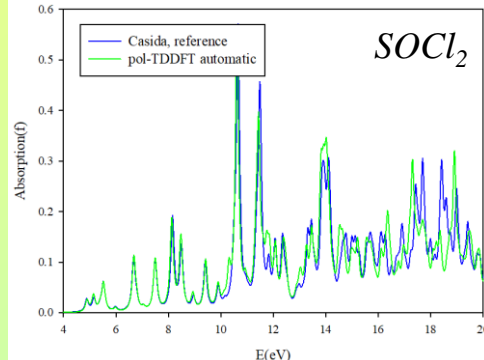
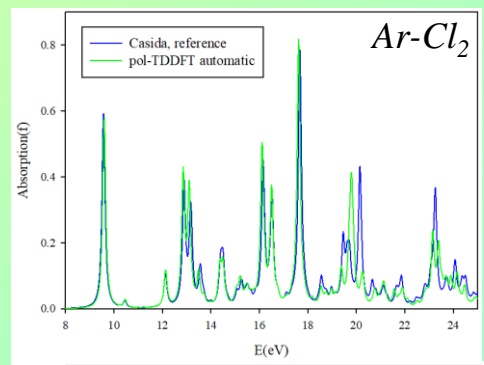
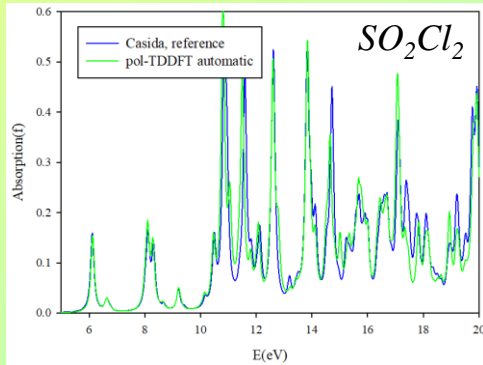
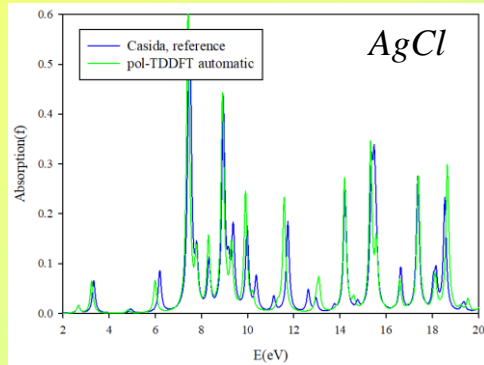
4S	$\alpha=5.12$
5S	$\alpha=4.51$
5S	$\alpha=3.29$
5S	$\alpha=2.40$
4P	$\alpha=8.31$
5P	$\alpha=4.28$
5P	$\alpha=2.80$
5D	$\alpha=3.75$
5D	$\alpha=2.40$
4F	$\alpha=5.00$
4F	$\alpha=3.00$

# Results and testing

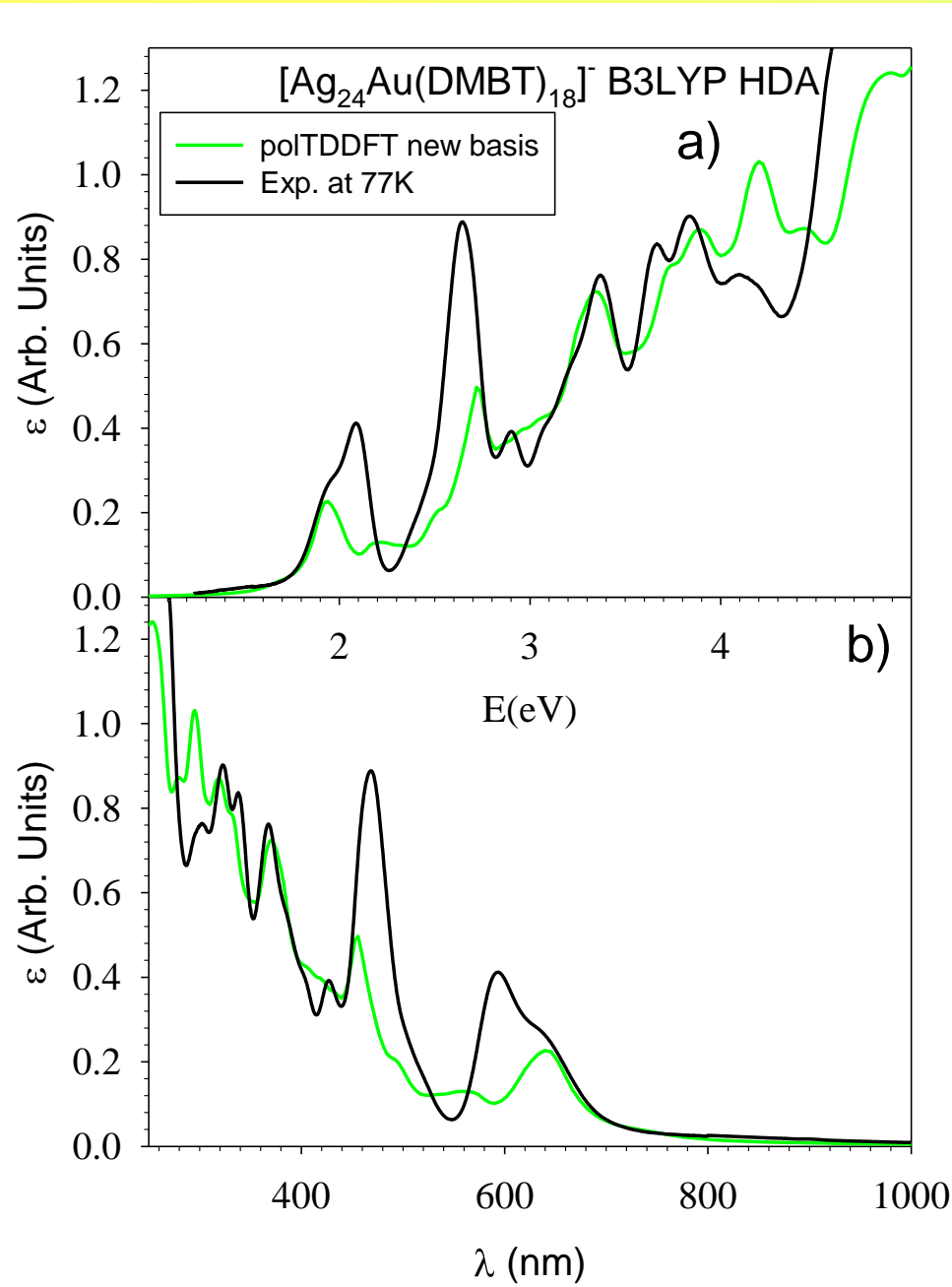
Inside the collection



Outside the collection



# Applications: $[\text{Ag}_{24}\text{Au}(\text{DMBT})_{18}]^-$ exp. at 77 K



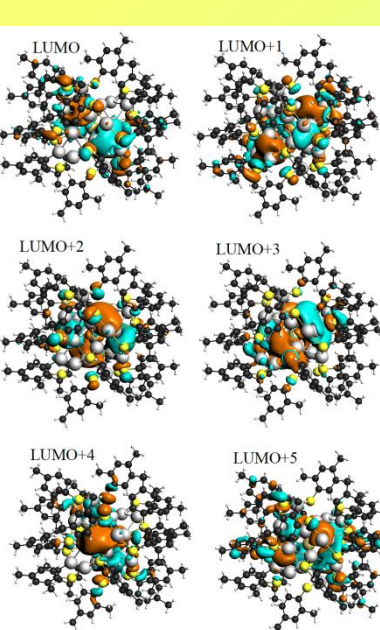
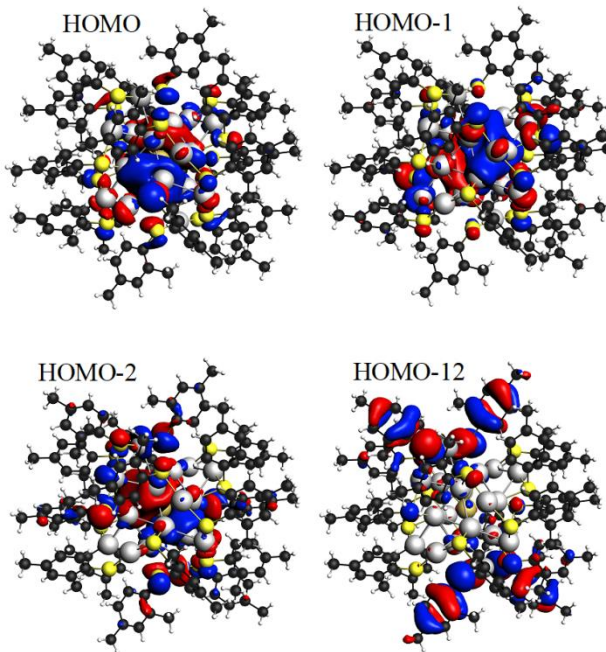
The photoabsorption data registered at 77K from the group of F. Maran in Padua.

In the low T spectrum emerge new features not visible at RT in excellent agreement with theory.

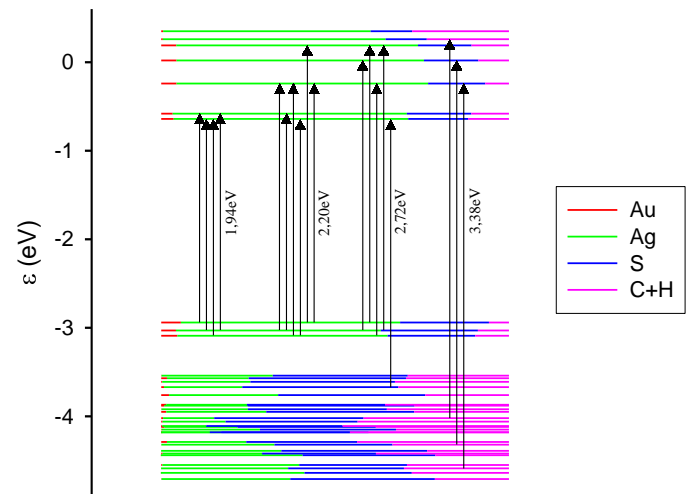
M. Medves, L. Sementa, D. Toffoli, G. Fronzoni, K. R. Krishnadas, F. Maran, T. Bürgi, A. Fortunelli, and M. Stener

“Predictive optical photoabsorption of  $[\text{Ag}_{24}\text{Au}(\text{DMBT})_{18}]^-$  via efficient TDDFT simulations”

J. Chem. Phys. 155 (2021) 084103



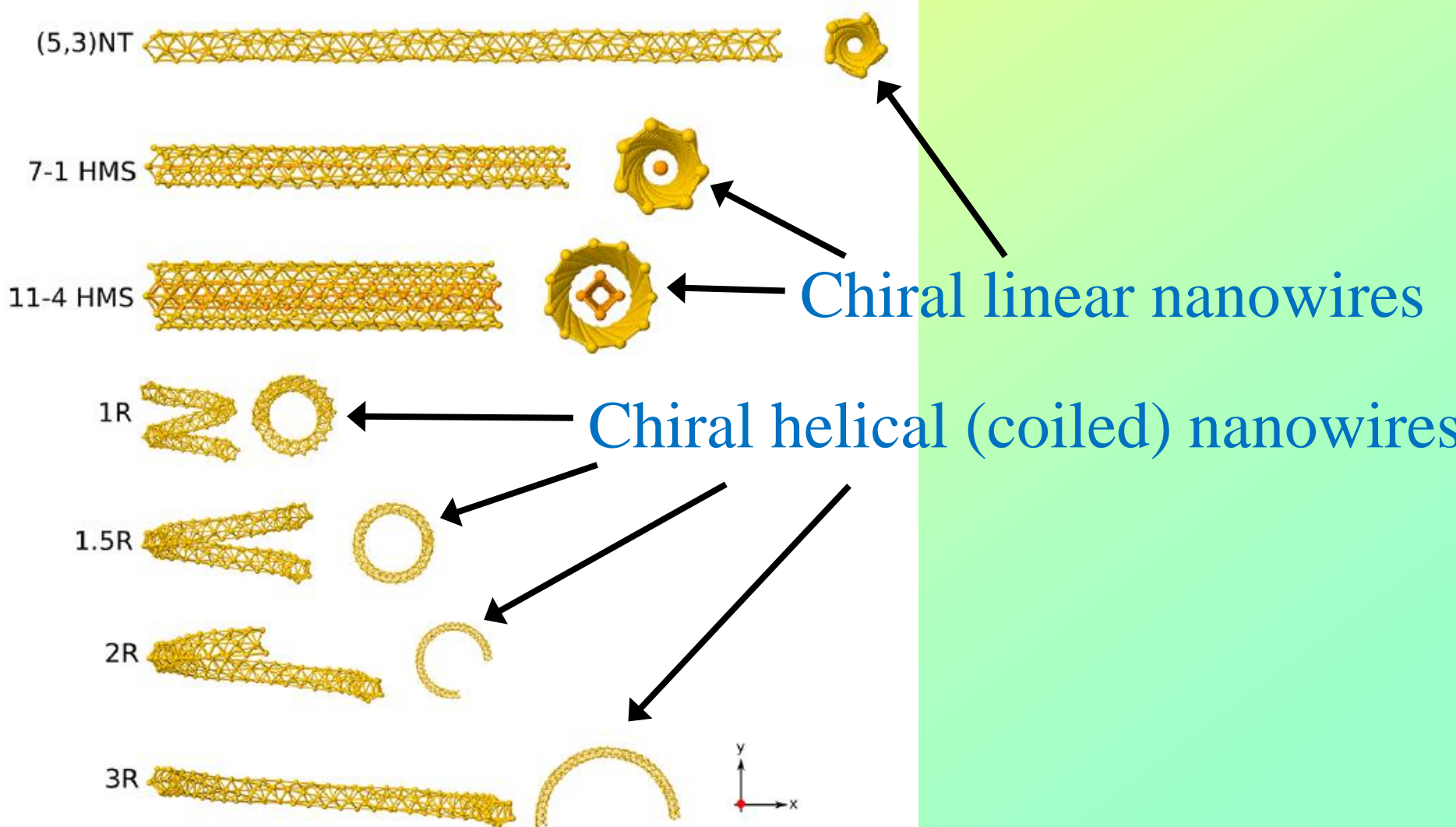
Inability of non-hybrid xc to describe the balance between metal and sulfur contributions. Tendency to move bands around the HOMO-LUMO gap to too low energies, thus underestimating the position of the corresponding excitations. Such excitations are blue-shifted and merged with higher-energy peaks when hybrid xc-functionals are employed



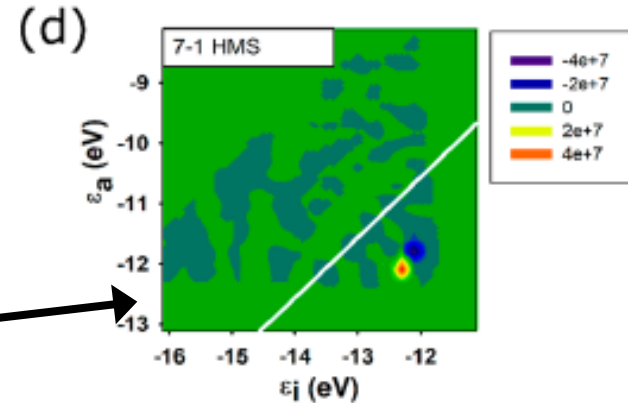
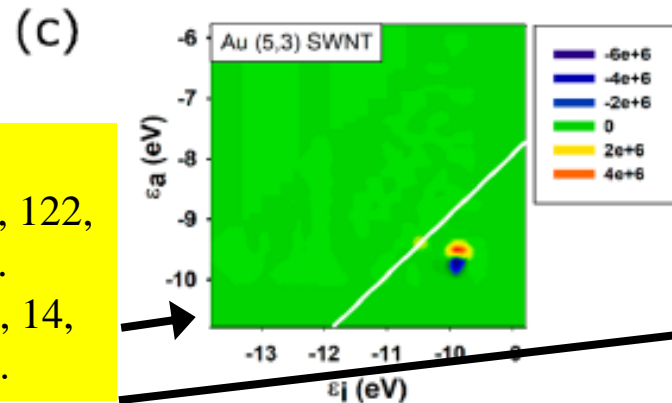
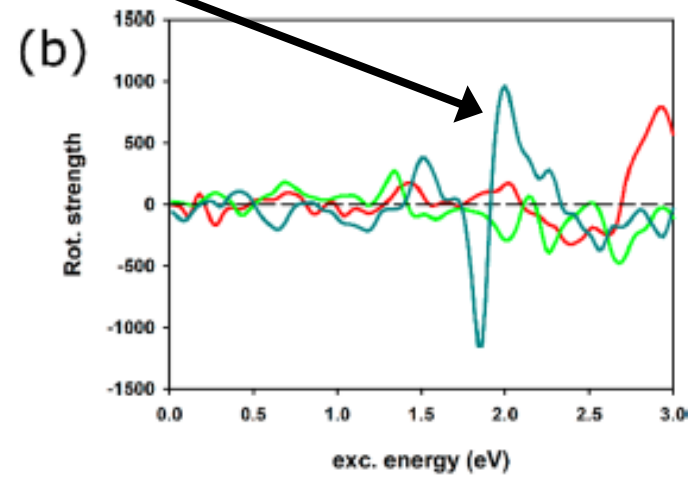
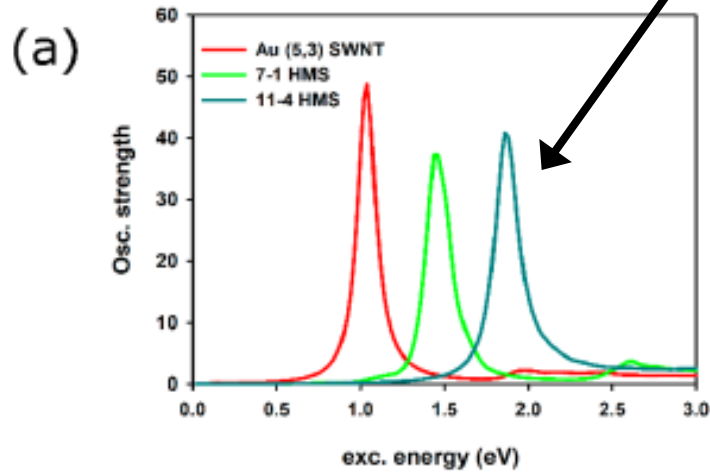
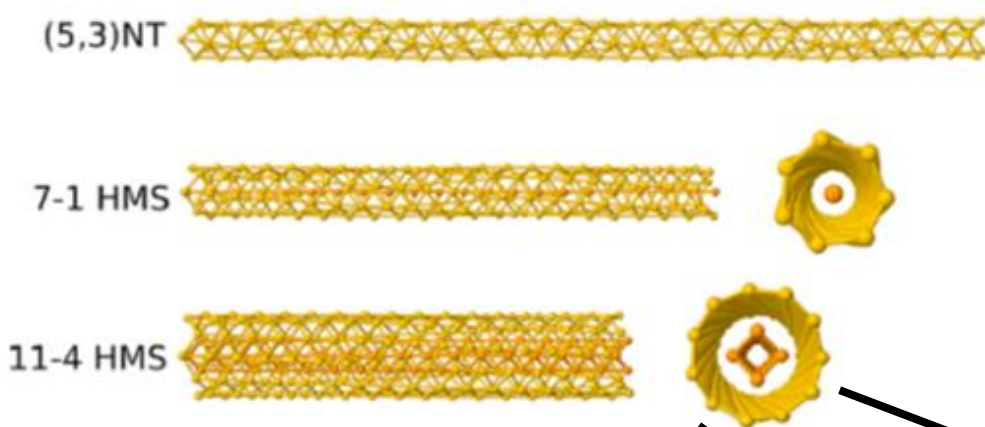
Transition energy (eV)	f	Assignment (only contribution > 10%)
1.94	0.23	21.7% HOMO (28% Ag 4s, 18% S 3p, 10% Ag 4p) → LUMO+1 (34% Ag 4s, 18% Ag 4p, 11% S 3p) 17.9 % HOMO-1 (27% Ag 4s, 20% S 3p) → LUMO (31% Ag 4s, 19% Ag 4p) 17.3% HOMO-2 (28% Ag 4s, 19% S 3p) → LUMO 16.7% HOMO-1 → LUMO+1
2.20	0.13	34.7% HOMO-1 → LUMO+2 (28% Ag 4p, 26% Ag 4s)
2.72	0.50	19.9% HOMO-1 → LUMO+3 (27% Ag 4s, 24% Ag 4p, 10% S 3p) 16.3% HOMO → LUMO+4 (25% Ag 4s, 24% Ag 4p)
3.38	0.72	11.5% HOMO-12 (37% S 3p, 18% C 2p) → LUMO+5 (31% Ag 4p)

# *Circularly Polarized Plasmons in Chiral Gold Nanowires via Quantum-Mechanical Design*

D. Toffoli, A. Russi, G. Fronzoni, E. Coccia, M. Stener, L. Sementa and A. Fortunelli, *J. Phys. Chem. Letters* 2021, **12**, 5829.

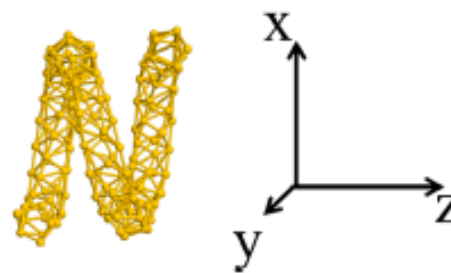
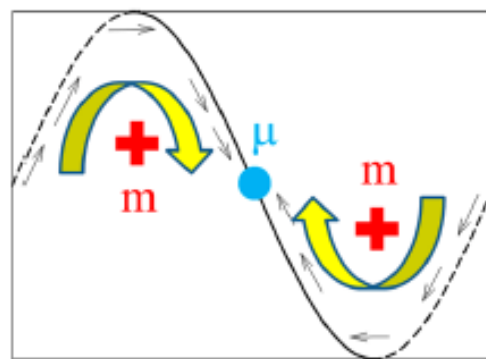
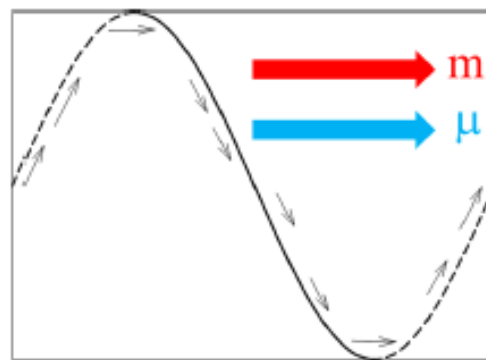
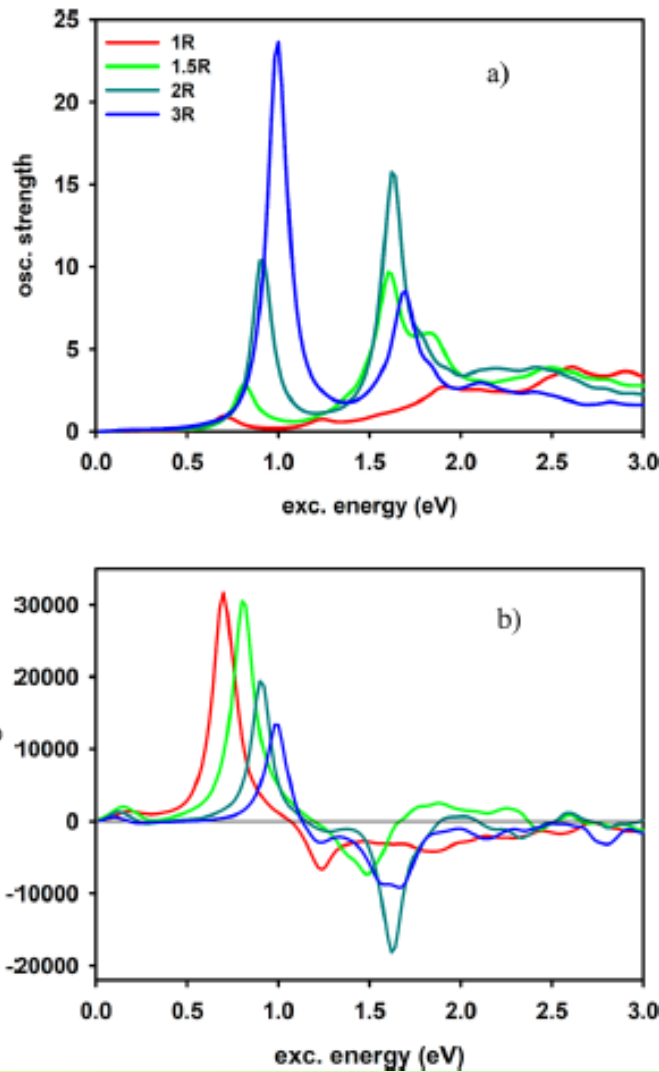


# Low Dichroism Plasmons for linear chiral nanowires, emerging in 11-4



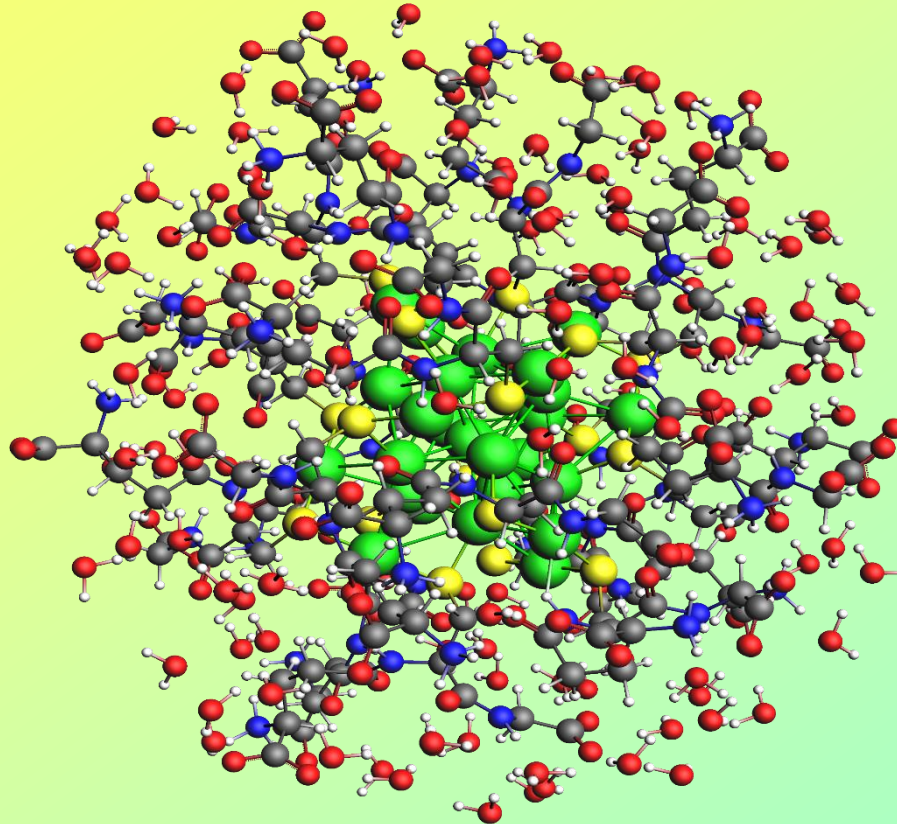
ICM plots:  
JPCC 2018, 122,  
4524–4531.  
JCTC 2018, 14,  
3703–3714.

# *Very large dichroism in plasmons for helical (coiled) chiral nanowires!*



Longitudinal and transversal plasmons with opposite dichroism

*Largest system considered so far: 1068 atoms, no symmetry, explicit solvent:  $[Au_{25}(GSH)_{18}]^{-1} \cdot (H_2O)_{126}$*



- Inclusion by MD and ED of conformational degrees of freedom for the calculations of ECD of chiral clusters

Marta Monti (HPC Europa3): Ongoing collaboration with S. Corni (Padua), M. Aschi (L'Aquila) and H. Hakkinen (Jyvaskyla)

## *Other applications*

- Calculation of transition moments between excited states and Real Time TDDFT  
P. Grobas-Illobre, M. Marsili, S. Corni, M. Stener, D. Toffoli and E. Coccia  
J. Chem. Theo. Comput. 17 (2021) 6314-6329
- Chiral functionalization of an atomically precise noble metal cluster: Insights into the origin of chirality and photoluminescence  
Krishnadas, Kumaranchira; Sementa, Luca; Medves, Marco; Fortunelli, Alessandro; Stener, Mauro\*; Fürstenberg, Alexandre; Longhi, Giovanna; Burgi, Thomas  
ACS Nano 14 (2020) 9687–9700
- Inclusion by MD and ED of conformational degrees of freedom for the calculations of ECD of chiral clusters  
Marta Monti (HPC Europa3): Ongoing collaboration with S. Corni (Padua), M. Aschi (L'Aquila) and H. Hakkinen (Jyvaskyla)
- More efficient HDA with Resolution of Identity (RI)  
Pierpaolo D'Antoni (HPC Europa3): Ongoing collaboration with L. Vissker (Amsterdam)
- Effect of O adsorption on optical (plasmon) properties of silver clusters  
Elena Zerbato (HPC Europa3): Ongoing collaboration with K. Neyman (Barcelona)

\$AMSBIN/ams << eor

## ***polTDDFT input for AMS***

ENGINESTART au170\_scf\_z2.t21

SYSTEM #1

Atoms

Au 2.786100 0.000000 -30.115689

(...)

End

Charge 2.0

END #1

TASK SINGLEPOINT #2

ENGINE ADF #3

Relativity

Formalism ZORA

Level scalar

End

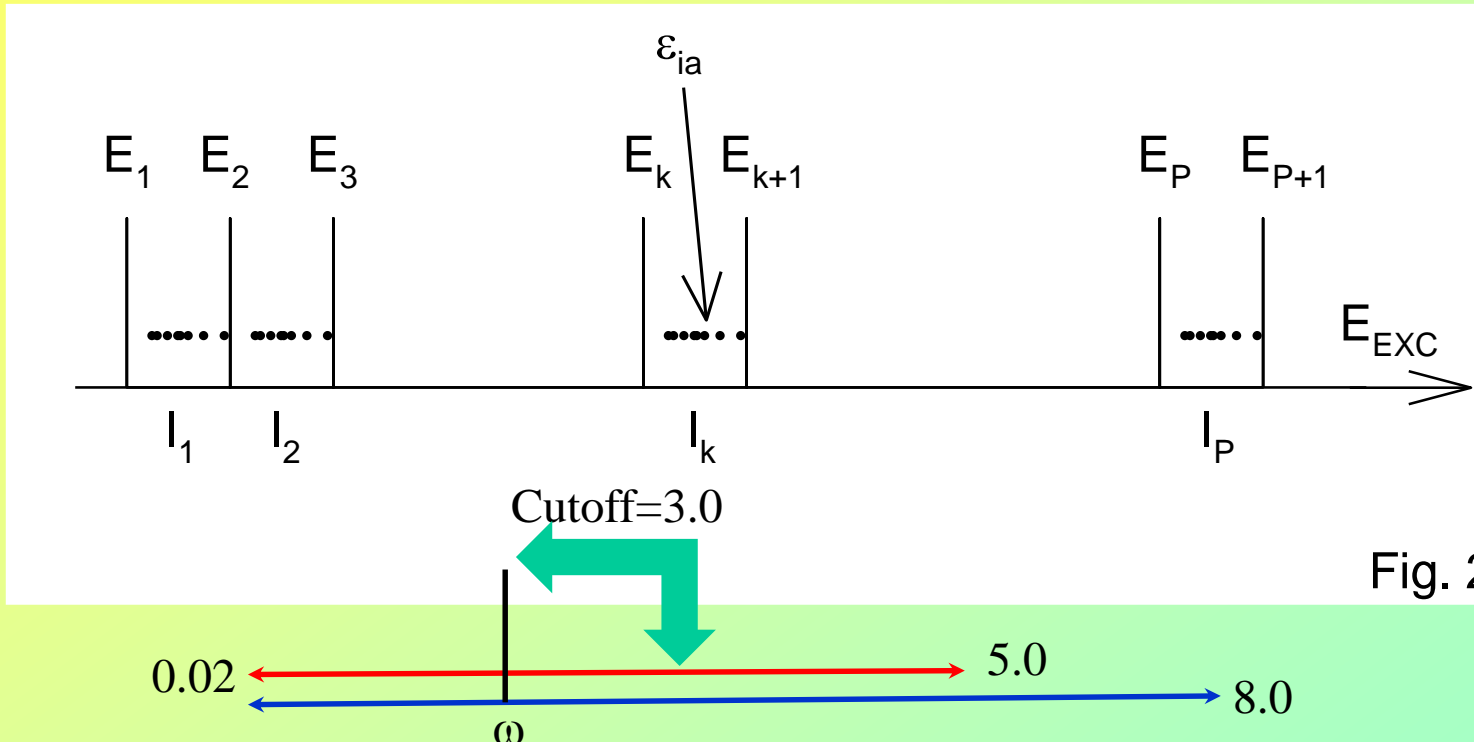
Basis

**PerAtomType Symbol=Au File=\$AMSRESOURCES/ADF/POLTDDFT/TZP/Au.4f**

End

(...)

# *polTDDFT input for AMS*



(...)

Poltdfft

FreqRange 0.02 5.02

### the spectrum is calculated from 0.0 to 5 eV

NFreq 249

### 249 points (step = (5.00-0.02)/249=0.02 eV)

KGrid 8.

### the excitations are calculated up to 8 eV ( $E_P$ )

NGrid 320

### 320  $I_k$  (width = 8/320=0.025 eV)

Lifetime 0.060

### imaginary photon energy (eV) = HWHM Lorentzian broadening

Cutoff 3.

### excitations are included up to  $\omega + \text{cutoff}$

End

(...) Cutoff: default 4 eV good for large systems, for small/medium systems cutoff may be increased up to 20 eV

Recommendation: check cutoff choice wrt a Casida calculation of the lowest part of the spectrum

# Conclusions:

- The density-matrix **Casida** approach is **not practical to treat big metal clusters**, since many roots (lowest eigenvalues) are necessary.
- The complex polarizability **polTDDFT** algorithm is proposed to treat large systems
- **Implementation** of the complex polarizability algorithm is completed in **AMS2021** code and published: JCP 143 (2015) 024106.
- **Hybrid XC** are the best choice in terms of agreement with experiment. But very demanding, **HDA** solves the problem (AMS2021)
- The **density fitting basis** set has been extended and reoptimized (**AMS2021**)
- All such new features are already available in AMS2022.
- The suggested protocol has proven predictive for alloyed MPC, further comparison with low T spectra for other systems will be necessary to confirm this conclusion in general.
- **Further extensions:** AMS2023: polTDDFT fast HDA RI, unrestricted HDA Casida, restarts options, ICM in GUI. AMS2024: unrestricted polTDDFT, RS functionals with RI in polTDDFT, improve parallelization.

# Acknowledgments:

Trieste University (Theory): **Giovanna Fronzoni, Daniele Toffoli, Emanuele Coccia, Marco Medves (PhD), Marta Monti (PhD), Pierpaolo D'Antoni (PhD, previous TCCM), Elena Zerbato (TCCM)**

ADF SCM group in Amsterdam: **Stan van Gisbergen, Erik van Lenthe, Fedor Goumans**

CNR Pisa (Theory and Metal clusters structure) : **Alessandro Fortunelli and Luca Sementa**

L'Aquila (MD and ED) : **Massimiliano Aschi**

Padova University (Low T photoabsorption exp.): **Sara Bonacchi, Tiziano Dainese, Flavio Maran (FF): Stefano Corni**

Jyvaskyla University (MD): **Hannu Hakkinen**

Lausanne University (Room T photoabsorption): **Kumaranchira Ramankutty Krishnadas, Thomas Bürgi**

**Thank you for your attention!**